Immunosuppression and Resultant Viral Persistence by Specific Viral Targeting of Dendritic Cells

By Noemí Sevilla,* Stefan Kunz,* Andreas Holz,* Hanna Lewicki,* Dirk Homann,* Hiroki Yamada,‡ Kevin P. Campbell,‡ Juan C. de la Torre,* and Michael B.A. Oldstone*

*From the *Department of Neuropharmacology, Division of Virology, The Scripps Research Institute, La Jolla, California 92037; and the ‡Department of Physiology and Biophysics, Howard Hughes Medical Institute, University of Iowa College of Medicine, Iowa City, Iowa 52242*

Abstract

Among cells of the immune system, $CD11c^+$ and DEC-205^+ splenic dendritic cells primarily express the cellular receptor (α-dystroglycan [α-DG]) for lymphocytic choriomeningitis virus (LCMV). By selection, strains and variants of LCMV that bind α-DG with high affinity are associated with virus replication in the white pulp, show preferential replication in a majority of $CD11c^+$ and DEC-205^+ cells, cause immunosuppression, and establish a persistent infection. In contrast, viral strains and variants that bind with low affinity to α-DG are associated with viral replication in the red pulp, display minimal replication in $CD11c^+$ and DEC-205^+ cells, and generate a robust anti-LCMV cytotoxic T lymphocyte response that clears the virus infection. Differences in binding affinities can be mapped to a single amino acid change in the viral glycoprotein 1 ligand that binds to α-DG. These findings indicate that receptor–virus interaction on dendritic cells in vivo can be an essential step in the initiation of virus-induced immunosuppression and viral persistence.

Key words: lymphocytic choriomeningitis virus • $CD11c^+$/DEC-205^+ cells • tropism • viral receptor • selection

Introduction

Understanding the mechanism by which viruses persist and escape immune surveillance is a key for defining measures to control and eliminate the infections and diseases they cause. Viruses that persist often interfere with the differentiated function of infected cells. This, in turn, could perturb the normal host homeostasis and lead to disease affecting the nervous, endocrine, immune, and other systems (1, 2). Some viruses that cause persistent infection associated with significant disease in humans are HIV, the agent of AIDS, EBV, hepatitis B virus, and hepatitis C virus (for a review, see reference 3).

Viruses that cause a persistent infection prevent the host's immune system from clearing the infectious agent. In many persisting infections of humans and animals, the infectious agent has been found in cells of the immune system (4). Dysfunction or destruction of such cells either directly by the virus or indirectly through immunopathologic mechanisms leads to immunosuppression. Therefore, it is important to determine the nature and expression pattern of the virus receptor on immune cells, as well as the contribution of the virus–receptor interaction to the resultant immunosuppression.

Lymphocytic choriomeningitis virus (LCMV)[1] can infect cells of the immune system, establish suppression of cellular and humoral immunoresponses, and cause persistent infection in its natural host, the mouse (5–8). Other studies identified the emergence and selection of a viral variant during the course of LCMV persistence that exhibited an immunosuppressive phenotype (7, 9–12). In vivo, this immunosuppressive variant becomes dominant over the nonimmunosuppressive parental virus in several tissues and cells, including those of the immune system (11–14). The parental virus, Armstrong (ARM) 53b, and the vast majority of viruses and variants isolated from the central nervous

Address correspondence to Michael B.A. Oldstone, Division of Virology, The Scripps Research Institute, 10550 N. Torrey Pines Rd., La Jolla, CA 92037. Phone: 858-784 8054; Fax: 858-784 9981; E-mail: mbaobo@scripps.edu

[1]*Abbreviations used in this paper:* aa, amino acid(s); APC, allophycocyanin; ARM, Armstrong; BHK, baby hamster kidney; CNS, central nervous system; Cl, clone; DC, dendritic cell; α-DG, α-dystroglycan; ECM, extracellular matrix; GP, glycoprotein; IDC, interdigitating dendritic cell; IS, immunosuppression phenotype; ko, knockout; LCMV, lymphocytic choriomeningitis virus; NP, nucleoprotein; P, persistence phenotype; RT, reverse transcriptase; S, small; VOPBA, virus overlay protein binding assay.

system (CNS) after intravenous inoculation of adult mice caused acute infections that were efficiently terminated within 7–10 d by the host anti-LCMV $CD8^+$ CTLs. In contrast, viral variants (>95%) isolated from lymphocytes and macrophages similarly injected into adult mice caused a generalized immunosuppression as judged by the absence of a primary CTL response to LCMV and other RNA and DNA viruses, and an inability to generate antibodies when immunized with soluble and particulate foreign antigens (8). It is the inability to generate a sufficient anti-LCMV CTL response, which is required to clear the virus, that leads to the development of a persistent infection.

LCMV is a negative-stranded RNA virus whose genome has two segments, a small (S) RNA and a large (L) RNA. The S RNA segment encodes the viral glycoprotein (GP) and nucleoprotein (NP), whereas the L RNA encodes the L and Z proteins. The GP is synthesized as a precursor protein (GPc) that is posttranslationally cleaved into GP1 (amino acids [aa] 1–264) and GP2 (aa 265–486). Sequence comparison between the prototypic immunosuppressive variant clone 13 (Cl 13) and the nonimmunosuppressive parental ARM 53b from which Cl 13 was derived showed five nucleotide changes. Only two of the changes caused aa substitutions (13, 15–17). One of these aa substitutions is in position 260 of GP1, with ARM 53b having F and Cl 13 L (F260L); the other aa change was in position 1079 of the L protein from K (ARM) to Q (Cl 13).

Recently, α-dystroglycan (α-DG) was identified as the receptor for LCMV (18). DG is a highly versatile cellular receptor for proteins of the extracellular matrix (ECM [19]). Key findings in the past few years demonstrated that DG plays a fundamental role in cell assembly and organization of basement membranes (for reviews, see references 20 and 21). Cl 13 was found to bind α-DG with higher affinity than ARM 53b (18). Competitive binding studies using soluble α-DG to block virus binding to cells expressing α-DG showed that viral reassortants made between Cl 13 and ARM 53b mapped attachment and infection of the virion to the S RNA segment (Tishon, A., and M.B.A. Oldstone, unpublished observations). As ARM 53b and Cl 13 have the same NP aa sequence, but differ at one single aa position in their GP, F260L in GP1 (16), these results implicated the GP1 mutation in binding of the virus to its cellular receptor. Consistent with this observation is the fact that only antibodies directed against GP1 exhibited neutralizing activity (22, 23).

Previous studies indicated that Cl 13 replicated in antigen-presenting interdigitating dendritic cells (IDCs), whereas ARM 53b showed limited replication in these cells (7). These findings raised four basic questions. First, is the phenomena observed between Cl 13 and ARM 53b generalizable to other LCMV isolates; second, do dendritic cells (DCs) preferentially express α-DG; third, do quantitative differences between viruses that bind at either high or low affinity to this receptor determine whether suppression of the immune response and resultant viral persistence occurs; and fourth, can specific molecular determinants in the virus GP1 account for differences in binding affinity to α-DG? Here we record three novel observations by characterizing the genome and determining the biology of 36 viral variants isolated from adult immunocompromised and persistently infected mice. First, viral variants causing immunosuppression (IS) and persistent (P) infection (IS^+P^+) routinely have a small aliphatic aa primarily in GP1 aa 260, L (20 out of 23 isolates) or I (3 out of 23 isolates), whereas in contrast, isolates that have a bulky aromatic aa (F) in GP1 aa 260 fail to cause both immunosuppression and viral persistence (IS^-P^-). Second, all IS^+P^+ virus variants bound to α-DG with at least 1 and most often 2–3 log higher affinity than did IS^-P^- viruses. Third, in vivo α-DG was preferentially expressed on DCs and not T, B, or $CD11b^+$ cells. The IS^+P^+ variants preferentially replicated in cells of the marginal zone and white pulp area in the spleen, whereas IS^-P^- viruses replicated in cells of the red pulp. Analysis of spleen cells infected by IS^+P^+ variants showed that they were IDCs ($CD11c^+$ and DEC-205^+ cells). Over the course of a 7-d in vivo infection there was a remarkable enhancement of infection of $CD11c^+$ and DEC-205^+ cells by IS^+P^+ viruses, with >50% of $CD11c^+$ cells and 17% of DEC-205^+ cells being infected. By 15 d, >80% of DEC-205^+ cells were also infected. In contrast, <1% of T and B lymphocytes and $CD11b^+$ cells were infected at similar time points. Taken in total, these findings implicate receptor–virus interaction on DCs in vivo as an essential step in the initiation of virus-induced immunosuppression and persistence.

Materials and Methods

Viruses and Mice Used. LCMV ARM 53b strain is a triple plaque-purified isolate of ARM CA 1371 (24) and was passaged in baby hamster kidney (BHK) cells. Cl 13 is a triple plaque-purified variant of ARM 53b derived from spleen cells of an adult BALB/WEHI mouse persistently infected since birth with ARM 53b (9). The isolation of LCMV WE clones c2.2 and c54 has been described (25). The new macrophage-, PBL-, CD4-, and CD8-derived LCMV viruses were isolated from purified populations (>99%) of T cells and macrophages obtained from $CD4^{-/-}$, $perforin^{-/-}$, and TNF-$\alpha^{-/-}$ gene–disrupted mice. The isolation of LCMV viruses was done by infectious center assay as described (26). All viral isolates were plaque purified three times; virus stocks grown in BHK cells and passage 1 or passage 2 levels were used in experiments. The plaque purification procedure, preparation of stock virus in BHK cells, and titration of viral stocks by plaquing has been described (9, 24). For virus overlay protein binding assay (VOPBA; reference 23), virus was concentrated and purified by precipitation with polyethylene glycol and renografin density gradient centrifugation (27).

BALB/c ByJ mice maintained and bred in The Scripps Research Institute were used for all experiments. These mice were infected as adults (7–10 wk old) by intravenous inoculation of 2×10^6 PFU of virus. $Perforin^{-/-}$, $CD4^{-/-}$, and TNF-$\alpha^{-/-}$ mice, as described (28, 29), had a mixed background of C57BL/6 and 129Sv. These mice were infected intracranially at birth with 10^3 PFU of ARM 53b.

Purification of Lymphocyte Subsets and Macrophages. PBLs were purified by Ficoll-Hypaque gradient centrifugation of mouse blood, as described (29, 30). In brief, heparinized blood was di-

luted in PBS, pH 7.2, layered into an equal volume of Ficoll-Hypaque solution (Sigma-Aldrich), and spun at 600 *g* for 15 min at room temperature. Cells at the interface were collected, washed in RPMI containing 10% FCS, and contaminating erythrocytes were removed by lysis with 0.83% ammonium chloride. $CD4^+$ and $CD8^+$ T cell subpopulations were isolated from spleen by FACS®. In brief, spleens were dispersed by pressing through a wire grid. Single-cell suspensions were marked using rat anti–mouse CD8-allophycocyanin (APC; BD PharMingen) and rat anti–mouse CD4-FITC (BD PharMingen) by incubating with the antibodies at 4°C for 20 min. The cells were washed three times with RPMI containing 5% FCS. After that, cells were sorted so that the purity of each subset was >99%. Isolation of peritoneal macrophages was done as described previously (31). In brief, C57BL/6 mice were injected with 3 ml of thyoglycollate (Becton Dickinson) 1 wk before isolation of macrophages. The macrophages were obtained by intraperitoneal lavage of the peritoneal cavity with PBS containing 1 mM EDTA. The preparation of macrophages was >99% pure as determined by staining with macrophage-specific monoclonal antibody F4/80 (32).

RNA Isolation, Nucleotide Sequence, and MnlI Digestion. Total RNA from BHK cells infected with the indicated viruses was isolated by the TRI reagent method (Molecular Research Center, Inc.). Purified RNA (1 μg) was transcribed to cDNA using 2 U of avian myeloblastosis virus reverse transcriptase (RT; GIBCO BRL) and then amplified by PCR using the Taq polymerase (Boehringer). The RT-PCR products were sequence by the fmol method (Promega).

MnlI digestion of 20 μl of the RT-PCR products was carried out, and the products were run on a 2% Seakem ME agarose gel (FMC Bioproducts) and visualized by ethidium bromide staining as described (11).

CTL Assay. The virus-specific CTL assay was quantitated by a standard ^{51}Cr-release assay (8, 9, 12). In brief, ^{51}Cr-labeled BALBCl7 cells ($H\text{-}2^d$) and MC57 cells ($H\text{-}2^b$), either uninfected or infected 48 h previously with ARM 53b at a multiplicity of infection of 1 PFU/cell, were employed as target cells. Effector cells were prepared from the spleens of individual mice 7–8 d after infection with 2×10^6 PFU intravenously with virus. Lysis was measured over a 5-h period at several effector/target ratios ranging from 50:1 to 5:1. Samples were set up in triplicate (variance was <10%). The results are expressed as the percentage of specific ^{51}Cr release: [(sample release − spontaneous release)/(maximum release − spontaneous release)] × 100. Lysis of uninfected targets mediated by effector cells has been subtracted from the infected cell value to give LCMV-specific lysis.

Serum Virus Titers. Serum virus titers were determined by plaque assay on Vero cell monolayers (9).

VOPBA. VOPBA was done as described (18, 23). In brief, purified α-DG was loaded on an SDS-PAGE, electrophoresed, and transferred onto nitrocellulose (0.45-μm pore size). The nitrocellulose was incubated overnight with purified virus (10^7 PFU). After several washes with PBS, 0.1% Tween 20, the nitrocellulose was incubated with monoclonal antibodies specific for LCMV GP. The proteins were detected with the enhanced chemiluminescence procedure according to the manufacturer's instructions (Amersham Pharmacia Biotech).

Riboprobe Generation. A 559-bp fragment of the LCMV NP was amplified by PCR of a NP cDNA using the primer pair 5′-CGGAATTCAGTCCATGAGTGCACAGTGC and 5′-CGGAATTCGAGAAACCTGCAGTCAATTC. A restriction digest with EcoRI was performed in the PCR fragment to subclone it into the EcoRI site of the pSP70 vector (Boehringer). After determining the orientation of the insert, a strand-specific LCMV NP riboprobe was synthesized using T7 RNA polymerase (Promega) in the presence of digoxigenin labeling mix (Boehringer [33]). An unrelated riboprobe labeled with digoxigenin and complementary to transcripts of the N protein of measles virus served as a negative control in this study and was synthesized as described previously (34). The amounts of synthesized riboprobes were determined by formaldehyde agarose gel electrophoresis.

In Situ Hybridization. Spleens from three to five animals for each experimental group were analyzed by in situ hybridization (33) 3 and 5 d after infection with various LCMV isolates. Tissue sections (6 μm thick) of fresh frozen tissue were collected on SuperFrost/Plus slides (Fisher Scientific) and fixed in 4% paraformaldehyde in phosphate buffer. Sections were acetylated by incubation in 0.1 M triethanolamine (Sigma-Aldrich), 0.25% acetic anhydride, subsequently treated with 0.1% Triton X-100/phosphate buffer, and prehybridized at room temperature in hybridization buffer (50% formamide [Sigma-Aldrich], 5× SSC, 2% blocking reagent [Boehringer]) for 2 h. Hybridization with digoxigenin-labeled riboprobes (50 ng/ml) was carried out overnight in hybridization buffer at 68°C. Sections were washed twice at room temperature with 2× SSC and twice at 70°C with 0.2× SSC for 30 min each. The digoxigenin-labeled riboprobe was then detected with an antidigoxigenin alkaline phosphatase conjugate (Boehringer) and NBT/BCIP color substrate (Boehringer). Developing times of the color reaction ranged from 4 to 10 h. Slides were counterstained with DAPI (Sigma-Aldrich), mounted in AquaMount (Fisher Scientific), and analyzed by light and UV microscopy.

Isolation of Splenic Cell Populations and Quantitation of LCMV-infected Cells. Cell suspensions were prepared from the spleens of mice infected 3, 5, 7, 15, and 20 d previously with various viral variants by mechanic disruption of the spleens. Cells were immunostained in PBS/2% (wt/vol) fetal bovine serum/0.2% (wt/vol) NaN_3 using as antibodies rat anti–mouse CD4-CyChrome, rat anti–mouse CD8-APC, rat anti–mouse B220-PE, rat anti–mouse CD11c-PE, and rat anti–mouse CD11b-APC (all from BD PharMingen). A rat anti–mouse DEC-205 antibody (Serotec) was used as primary antibody, and as a second antibody PE-labeled $F(ab')_2$ mouse anti–rat IgG (Caltag) was used. After staining, cells were fixed and permeabilized in PBS/1% fetal bovine serum (wt/vol)/4% paraformaldehyde (vol/vol)/0.1% saponin (wt/vol). Affinity-purified antibody to LCMV NP (113) was conjugated to Alexa-488 according to the protocol recommended by the manufacturer (Molecular Probes) and used for intracellular detection of LCMV NP. Cells were acquired using a FACSCalibur™ flow cytometer (Becton Dickinson). Dead cells were excluded on the basis of forward and side light scatter. Data were analyzed using CELLQuest™ software (Becton Dickinson).

Isolation of α-DG from Splenic Cell Populations. Splenic cell populations were prepared from naive mice by mechanical disruption of the spleens. Cells were immunostained in HBSS (GIBCO BRL)/1% (vol/vol) fetal bovine serum/1.2 mM EDTA containing protease inhibitors (Boehringer) using antibodies rat anti–mouse CD11c-biotin, rat anti–mouse CD4-CyChrome, rat anti–mouse CD8-APC, and rat anti–mouse B220-PE (all from BD PharMingen). After staining, the splenocytes were incubated with Dynabeads M-280 Streptavidin (Dynal). The Dynabeads coated with biotinylated CD11c were separated using a Dynal Magnetic Particle Concentrator (MPC) for 2–3 min. The unbound cells were sorted by FACS® to insure purity of >98%. The different cell populations ($CD11c^+$, $CD4^+$, $CD8^+$, $B220^+$,

Table I. *Characterization of LCMV Isolates Used in This Study*

Virus isolate*	Carrier mouse‡	LCMV-specific CTLs in spleen§ (E/T ratio of 50:1)	LCMV titer (PFU) per ml of serum (15/30 d)	aa position 1079 of L‖	aa position 260 of GP¶
ARM 53b		80	<50	K	F
Cl 13		0	$1 \times 10^5/3 \times 10^4$	Q	L
Mac 13-3	CD4 ko mice	0	$2 \times 10^5/1 \times 10^5$	K	L
Mac 14-1	150 d after infection	0	$1 \times 10^6/2 \times 10^5$	K	L
PBL 7-1		0	$3 \times 10^5/1 \times 10^6$	K	L
PBL 6-4		0	$1 \times 10^4/2 \times 10^5$	N	L
PBL 36-1	Perforin ko mice	2.2	$1 \times 10^3/2 \times 10^4$	N	L
PBL 36-2	7 mo after infection	0	$1 \times 10^4/1 \times 10^3$	N	L
PBL 36-3		0.6	$5 \times 10^6/2 \times 10^2$	N	L
PBL 36-4		6	$3 \times 10^4/1 \times 10^3$	N	L
PBL 50-1		4.6	$9.5 \times 10^4/1 \times 10^3$	K	I
PBL 50-2		0	$3.3 \times 10^3/1 \times 10^2$	K	I
PBL 50-3		0	$6 \times 10^4/1.5 \times 10^2$	K	I
PBL 66-1		0	$5.3 \times 10^3/3.3 \times 10^2$	K	L
PBL 66-2		0	$1.7 \times 10^4/<50$	K	L
PBL 66-3		0	$5 \times 10^5/2 \times 10^2$	K	L
PBL 67-3		0	$2.1 \times 10^5/1 \times 10^4$	Q	L
PBL 67-4		0	$1.4 \times 10^4/5 \times 10^2$	Q	L
CD8-4	Perforin ko mice	60	<50	K	F
CD8-5	24 d after infection	78	<50	K	F
CD8-6		80	<50	K	F
CD8-7		80	<50	K	F
CD8-8		73	<50	K	F
CD4-1		60	<50	K	F
CD4-2		63	<50	K	F
CD4-5		80	<50	K	F
TNCD8-1	TNF-α ko mice	0	$2 \times 10^2/1 \times 10^2$	ND	L
TNCD8-2	3 mo after infection	0	$3 \times 10^4/2 \times 10^4$	ND	L
TNCD4-1		0	$3 \times 10^3/2 \times 10^4$	ND	L
TNCD4-2		0	$1.1 \times 10^4/2 \times 10^2$	ND	L
TNPBL2-1		0	$2 \times 10^2/<50$	ND	L
TNPBL2-2		0	$2 \times 10^3/3 \times 10^2$	ND	L
TNPBL4-1		11	$4 \times 10^3/2 \times 10^2$	ND	L
TNPBL4-2		0	$3 \times 10^4/<50$	ND	L
TNB4-1		48	<50	ND	F
TNB4-2		80	<50	ND	F
TNB2-1		78	<50	ND	F
TNB2-2		60	<50	ND	F

BALB/c ByJ mice were infected intravenously with 2×10^6 PFU of isolated virus. The CTL response was checked at day 7 after infection and viral titers in sera were measured at days 15 and 30 after infection. The data shown are the averages of values from two to four mice per group.
*Virus isolates were obtained by picking plaques formed by macrophages (Mac), $CD4^+$ cells (CD4), $CD8^+$ cells (CD8), PBLs, and brain homogenate (TNB). TNCD8, TNCD4, and TNPBL refer to isolates from $CD8^+$, $CD4^+$ cells, and PBLs, respectively, of TNF-α ko mice.
‡These virus isolates had been selected in immunocompromised mice (CD4 ko, perforin ko, and TNF-α ko) at different times after inoculation.
§These values are percentages of ^{51}Cr release from BALB/c Cl7 (H-2d) targets at an E/T ratio of 50:1.
‖The cDNA that encodes aa 1079 of the L gene was amplified by PCR and the PCR product was sequenced as described in Materials and Methods.
¶The aa at position 260 of GP1 was checked by the RT-PCR MnlI digestion technique described in Materials and Methods. The RT-PCR products were sequenced.

and total splenocytes) were lysed in 50 mM Hepes, pH 7.5/200 mM NaCl/5 mM $MgCl_2$/5 mM $CaCl_2$/1% (wt/vol) NP-40/1.2 mM EDTA/1 mM PMSF for 45 min on ice. After centrifugation for 10 min at 14,000 rpm, the supernatants were incubated with 20 μl of jacalin coupled to agarose (Vector Laboratories) overnight at 4°C. The matrix was washed three times in lysis buffer, and the eluted proteins were resolved in a 6% SDS-polyacrylamide gel for VOPBA with 10^8 PFU of LCMV Cl 13. α-DG from MC57 cells was isolated using the same procedure.

Results

Characterization of LCMV Isolates from Immune and CNS Cells of Persistently Infected Mice. To evaluate the consequence of selection by immune pressure on the viral quasispecies generated in a persistently infected mouse, we isolated viruses from mice immunocompromised by disruption of either CD4, perforin, or TNF-α genes. LCMV ARM 53b was used to initially infect each group of knockout (ko) mice. Viruses were recovered by cocultivation on permissive Vero cells from purified populations (>99% pure) of individual $CD4^+$ and $CD8^+$ T cells, macrophages, and PBLs. Cell populations were purified using monoclonal antibodies and flow cytometry. In addition, viruses were isolated from the CNS of such persistently infected mice. Such viruses persist and replicate exclusively in neurons (35, 36). Isolated viruses were three times plaque purified, and their biological properties were evaluated by two criteria: (a) the ability to elicit an LCMV-specific CTL response at day 7–8 after infection, and (b) their ability to cause a persistent infection in vivo. For these studies, a minimum of three mice were challenged with each clonal virus isolate. The results indicated that viruses isolated from lymphocytes or macrophages obtained from CD4, perforin, and TNF-α ko mice persistently infected for at least 7 mo failed to generate LCMV-specific CTL responses and caused a persistent infection (Table I). These viruses are referred to as CTL^-P^+. In contrast, viruses isolated from the CNS of TNF-α ko mice elicited a potent LCMV-specific CTL response, which cleared the virus within 2 wk and left no evidence of persistent infection. These viruses are referred to as CTL^+P^-. Interestingly, viruses isolated from $CD4^+$ and $CD8^+$ cells within the first 24 d of the persistent infection showed the same phenotype (CTL^+P^-) as the parental ARM 53b (Table I).

An Aliphatic aa at Position 260 of the Viral Glycoprotein Is Associated with the CTL^-P^+ Phenotype of LCMV Variants. To identify the genetic changes of the CTL^-P^+ viruses, the sequence of the viral GP and selected regions of the viral polymerase (L) was determined using two independent strategies. First, to determine the aa in 260 of GP1, an initial screen using a cDNA copy of isolated viral RNA, treated with MnlI enzyme and gel electrophoresis (11), was employed followed by direct sequencing of the entire GP1. Both the MnlI screen and direct sequencing indicated that the vast majority (21 out of 24) of CTL^-P^+ viruses had an L at 260 of GP. In contrast, those viruses with the phenotype CTL^+P^- (12 out of 12) had an F at this aa position. Three CTL^-P^+ variants, PBL 50-1, PBL 50-2, and PBL 50-3, did not show the expected 202- and 160-bp fragments after MnlI digestion of the corresponding 362-bp PCR products (11). Sequence analysis of these three viruses indicated that they possessed a different aliphatic aa, I, at position 260 of GP1. Sequence analysis of GP1 from both CTL^-P^+ and CTL^+P^- variants showed that several viruses exhibited additional changes to the one in position 260 (data not shown). However, of all these viruses showed the same CTL^-P^+ phenotype as those with the single aa substitution F260L. Thus, it seems unlikely that the additional changes contributed to the CTL^-P^+ phenotype.

The change K1079Q in the L protein did not correlate with the CTL^-P^+ phenotype (Table I). These data suggest that any role played by the polymerase in the CTL^-P^+

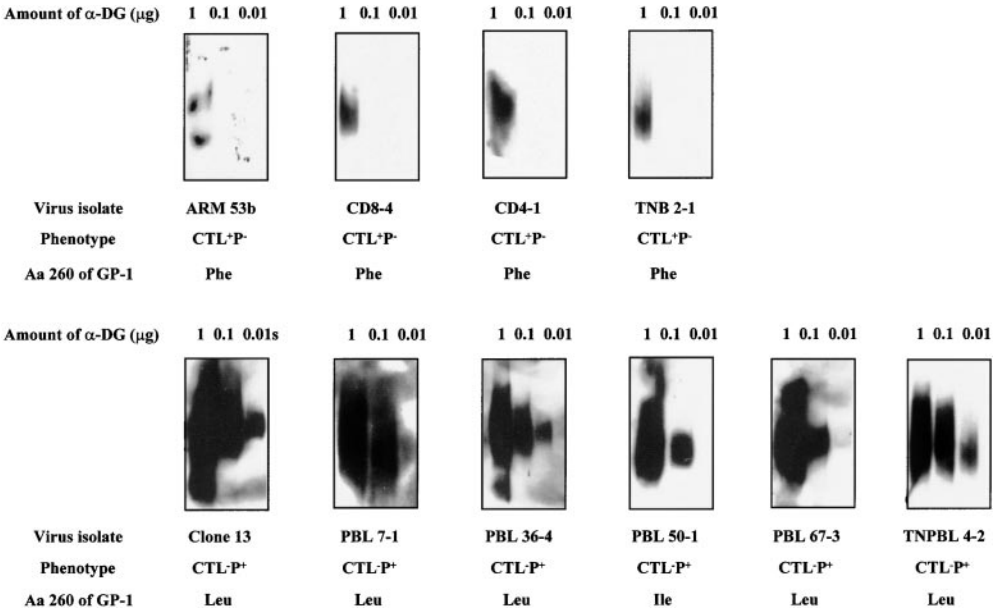

Figure 1. VOPBA with purified α-DG and LCMV variants. Decreasing amounts (1, 0.1, and 0.01 μg) of purified α-DG were incubated with 10^7 PFU of each viral isolate and then with virus-specific antibody as described in Materials and Methods. The top panels show the VOPBA of CTL^+P^- LCMV isolates (ARM 53b, CD8-4, CD4-1, and TNFB2-1). The phenotype as well as the aa in position 260 of GP1 (F) is shown under each blot. The bottom panel shows the VOPBA of CTL^-P^+ LCMV isolates (Cl 13, PBL 7-1, PBL 36-4, PBL 50-1, PBL 67-3, and TNPBL4-2). The CTL P phenotype is indicated under the name of each isolate and the aa in position 260 of GP1 (L or I).

phenotype does not map specifically to aa position 1079. It is plausible that other aa positions within the L protein could contribute to the CTL^-P^+ phenotype. Nevertheless, reassortants made between Cl 13 (CTL^-P^+) and parental ARM 53b (CTL^+P^-) viruses that differ only in two positions, one in GP 260 (F260L) and the other in the L (K1079Q), indicated that both the CTL^-P^+ phenotype (12) and the binding and infection of α-DG^+ cells mapped to the S RNA of Cl 13 (Tishon, A., and M.B.A. Oldstone, unpublished observations). The S RNA encodes the viral NP that is identical between Cl 13 and ARM, and the viral GP that differs in a single aa, thus strongly suggesting that the mutation in the GP but not in the polymerase is likely to be important for the CTL^-P^+ phenotype. As this biologically important aa mutation occurred in the segment of GP (GP1) implicated in binding to the virus receptor, we turned our attention to the analysis of virus–α-DG binding.

High Affinity Binding of Viral Variants to the α-DG Receptor Correlates Directly with the CTL^-P^+ Phenotype. To establish the role of aa 260 in the binding to α-DG, several virus isolates with either a CTL^-P^+ or a CTL^+P^- phenotype were quantitatively assayed for their binding affinity to α-DG. All LCMV variants with an L or I in position 260 of GP1 showed high binding affinity to α-DG, comparable to that of Cl 13, with binding of at least 1 log and often 2–3 logs greater than that observed with CTL^+P^- viruses that contained F at GP1 aa 260 (Fig. 1). Competitive inhibition binding assays using soluble α-DG and 10 different viral strains or variants showed that high affinity virus binders were routinely blocked by 1–4 nM soluble α-DG (33% blocking) whereas in contrast, low affinity viral binders re-

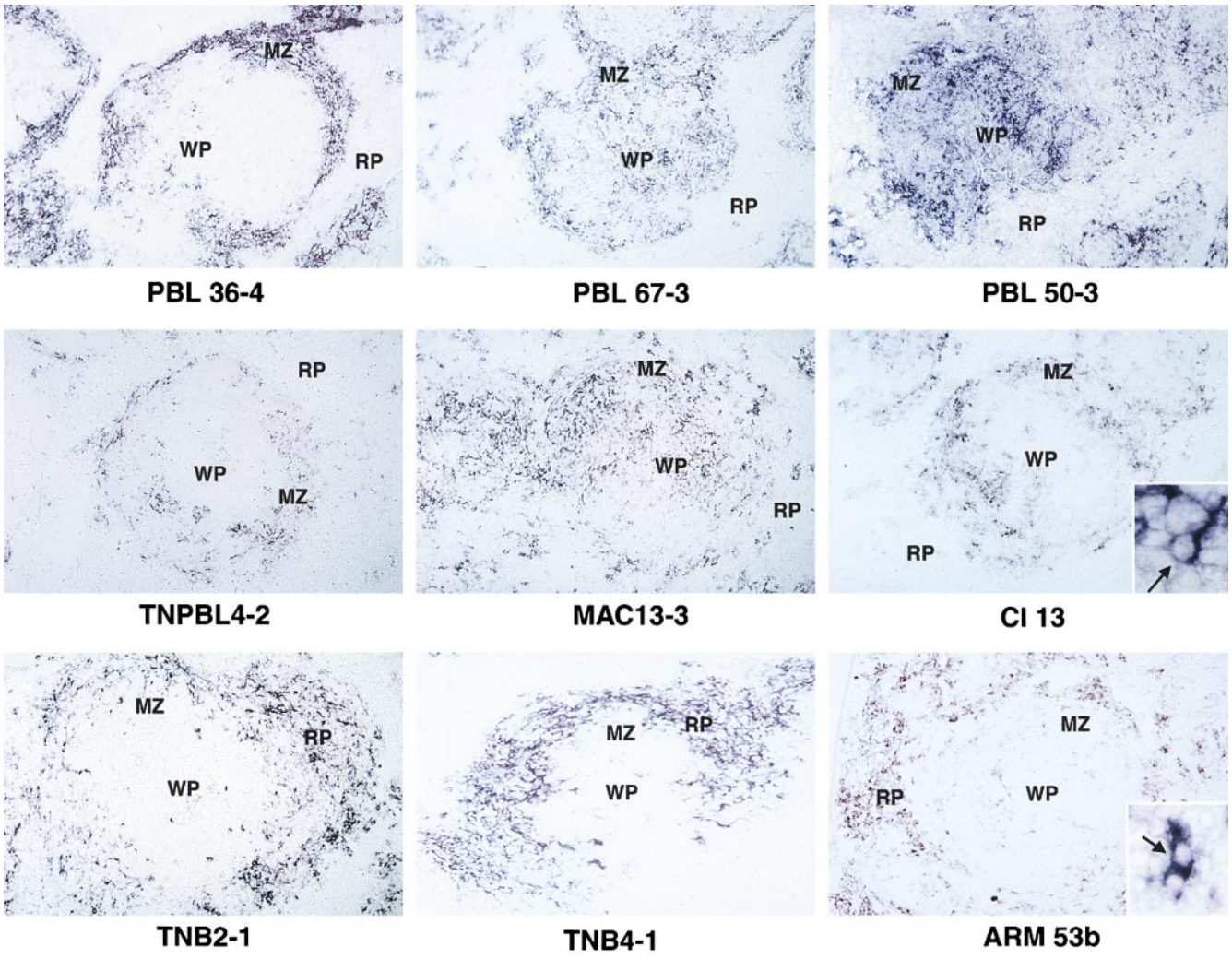

Figure 2. Anatomic locations of viral nucleic acids within the spleen 3 d after infection with LCMV ARM 53b, Cl 13, and representative CTL^-P^+ (PBL 36-4, PBL 67-3, PBL 50-3, TNPBL4-2, and Mac 13-3) and CTL^+P^- variants (TNB2-1 and TNB4-1) of ARM 53b. In situ hybridization was performed using a digoxigenin-labeled riboprobe specific for LCMV NP. In spleen sections from BALB/c ByJ mice infected intravenously with 2×10^6 PFU of virus ARM 53b, TNB2-1, or TNB4-1, the nucleic acids localized predominantly in the red pulp (RP). Using identical conditions, the nucleic acids of CTL^-P^+ virus isolates localized within the white pulp (WP) or its marginal zone (MZ). All panels are shown at the same magnification. A higher power view is shown in the inset for ARM 53b– and Cl 13–infected mice. The arrows indicate viral nuleic acid detected in individual cells.

quired >400 nM soluble α-DG to block binding to α-DG cells (data not shown). Taken together, these findings indicated that an aliphatic aa–like L or I in position 260 of GP1 of LCMV viruses is associated with high affinity binding to α-DG, whereas those viruses containing an aromatic (F) aa at this position bound at least 1 and most often at 2–3 logs lower affinity to α-DG.

High Affinity Binding CTL$^-$P$^+$ Variants Preferentially Replicate in CD11c$^+$ and DEC-205$^+$ Cells Located in the White Pulp of the Spleen. Next, we analyzed the anatomic distribution of CTL$^-$P$^+$ and CTL$^+$P$^-$ viruses in the spleens of adult immunocompetent mice infected 3 d previously with 2×10^6 PFU of virus intravenously. For these studies, four sections from at least four independently inoculated mice were examined using a digoxigenin-labeled probe to LCMV NP and in situ hybridization. The results indicated that CTL$^-$P$^+$ viruses localized exclusively in cells of the marginal zone and white pulp (Fig. 2). In contrast, CTL$^+$P$^-$ variants localized primarily to cells within the red pulp (Fig. 2). By 5 d after infection, the spleens from mice infected with CTL$^-$P$^+$ viruses exhibited the beginning of an extensive destruction of lymph follicle structures similar to previous reports (7, 37). Infection with the CTL$^+$P$^-$ viruses had no such effect (data not shown).

To identify specific cells in the spleen that were infected by LCMV, suspensions of single cells prepared from individual spleens were labeled with specific monoclonal antibodies to cell surface markers coupled to a fluorochrome probe. This was complemented with the use of an antibody to LCMV NP directly coupled to a different and distinct fluorochrome, thereby allowing detection of viral antigen in the specifically marked cell type. CTL$^-$P$^+$ viruses primarily infected CD11c$^+$ (cellular marker of most DCs in mouse lymphoid tissue [38]) and DEC-205$^+$ (antigen expressed on interdigitating DCs in lymphoid tissues [39]) cells with only minimal to negligible infection of CD11b$^+$, B220$^+$, CD4$^+$, and CD8$^+$ cells, as indicated in the graph and a summary of the experiments shown in the table under the graph in Fig. 3 B. In contrast, as shown in Fig. 3 A, there was minimal infection of both CD11c$^+$ and DEC-205$^+$ cells by the CTL$^+$P$^-$ viruses. We next quantified the number of CD11c$^+$ and DEC-205$^+$ cells infected and determined the in vivo replication kinetic over the first 20 d of infection. At day 7 after infection, 60% of CD11c$^+$ cells and 17% of DEC-205$^+$ cells were infected with CTL$^-$P$^+$ viruses. Thereafter, the number of DEC-205$^+$ cells infected by CTL$^-$P$^+$ viruses markedly increased over the next week so that by day 15, >80% of DEC-205$^+$ cells contained LCMV antigens (Fig. 4, A and B, show results from mice infected with Cl 13). In contrast, significantly fewer CD11c$^+$ and DEC-205$^+$ cells were infected by CTL$^+$P$^-$ viruses (Fig. 4 B shows results from mice infected with ARM 53b). Over the 20-d observation period, <1% of CD4$^+$, CD8$^+$, B220$^+$, and CD11b$^+$ cells were infected with CTL$^-$P$^+$ or CTL$^+$P$^-$ viruses. These data indicate: first, that DCs are the primary cell infected in vivo by CTL$^-$P$^+$ LCMV variants; second, that CTL$^-$P$^+$ viruses astoundingly infect >50% of CD11c$^+$ and DEC-205$^+$ cells but <1% of CD11b$^+$, B, CD4, and CD8 T lymphocytes; and third, that CTL$^+$P$^-$ viruses fail to infected significant numbers of DCs. Thus, viral variants with a CTL$^-$P$^+$ phenotype bound with high affinity to the α-DG receptor and

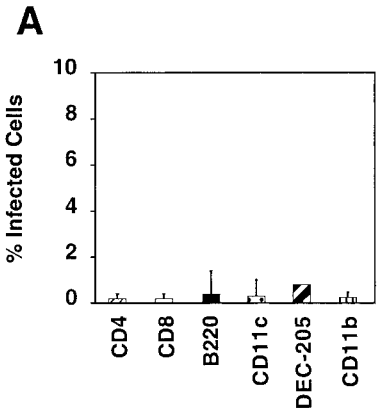

Virus	% APC (CD11c$^+$ & DEC-205$^+$)	% Other Cells
ARM 53b	1	0.6
TNFB2-1	1	0.3
TNFB4-1	2	0.3

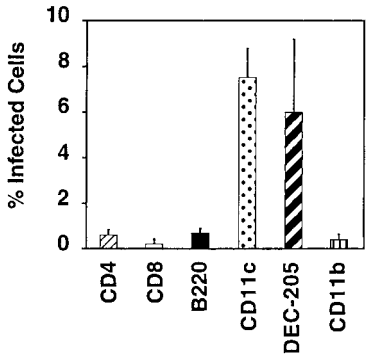

Virus	% APC (CD11c$^+$ & DEC-205$^+$)	% Other Cells
Clone 13	9	0.8
Mac 13-3	12	0.5
PBL 7-1	10	0.4
PBL 36-4	9	0.6
PBL 67-3	20	0.2
TNFPBL4-1	9	0.3

Figure 3. Comparative levels of infectivity in immune cells caused by CTL$^-$P$^+$ and CTL$^+$P$^-$ viral variants. In each experiment, four adult BALB/c ByJ mice were injected intravenously with 2×10^6 PFU of virus, and 3 d after infection a pooled splenocyte suspension was prepared from each mouse (see Materials and Methods). Each cell population was labeled with cell-specific monoclonal antibodies to CD4, CD8, B220, CD11c, DEC-205, and CD11b. Subsequent intracellular staining using specific antibody to LCMV NP (antibody 113) was performed, followed by FACS®. The graph represents percentages of cells in each subset infected with ARM 53b (A) or Cl 13 (B). Summarized below are the percentages of infected antigen-presenting cells (CD11c, CD11b, B220, and DEC-205$^+$ cells) or CD4 and CD8 T cells infected with these viruses. The term "other cells" refers to the sum of percentages for infected CD11b$^+$, B220$^+$, CD4$^+$, and CD8$^+$ T cells. (A) Infection of cell populations by CTL$^+$P$^-$ viruses. (B) Infection of cell populations by CTL$^-$P$^+$ viruses.

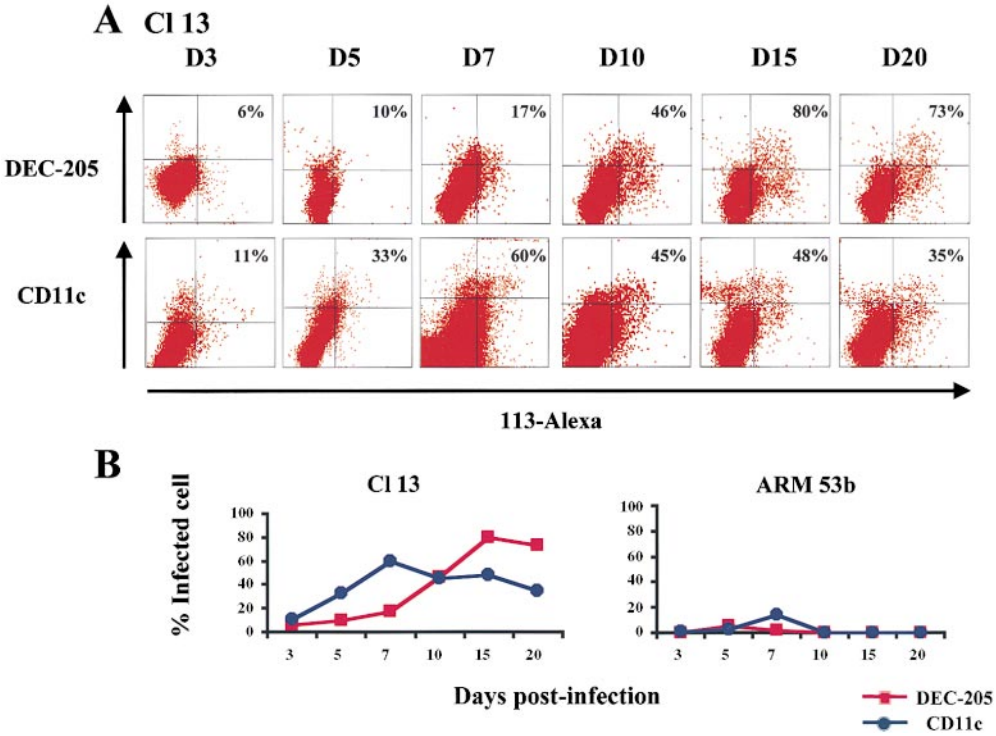

Figure 4. Replication of CTL$^-$P$^+$ and CTL$^+$P$^-$ viruses in DCs. Four adult BALB/c ByJ mice were infected intravenously with 2×10^6 PFU of either ARM 53b or Cl 13. CD11c$^+$ and DEC-205$^+$ cells obtained from pooled spleens made into single splenocyte suspensions were labeled with specific antibodies for these cell subsets (see Materials and Methods). (A) Replication of Cl 13 in DCs. After intracellular staining with the monoclonal antibody specific to LCMV NP (113) and FACS®, dot plots were obtained that showed double-positive cells for 113-Alexa and DEC-205$^+$ (top) or CD11c$^+$ (bottom) cells. The numbers in each dot plot denote the percentage of 113-Alexa$^+$ cells over the background in each cell population. (B) Curve plots show the replication of Cl 13 and ARM 53b in DEC-205$^+$ and CD11c$^+$ cells over a 20-d observation period.

preferentially infected DEC-205$^+$ and CD11c$^+$ cells of the marginal zone and white pulp in the spleen. This phenotype is referred to as IS$^+$P$^+$. LCMV variants that failed both to suppress immune responses and to establish persistence are referred to as IS$^-$P$^-$.

Identification of a Second aa Site in GP1 Associated with the IS$^+$P$^+$ Phenotype. In the next series of experiments, we evaluated whether another strain of LCMV, WE, which has 94% identity at the aa level with ARM 53b or Cl 13 (25), exhibited the same correlation between immunosuppression, viral persistence, high affinity binding to α-DG, and preferential infection of CD11c$^+$ and DEC-205$^+$ cells in the white pulp. Two clonal isolates of the LCMV-WE54 parental strain, WE c2.2 and WE c54, were analyzed. Inoculation of adult immunocompetent mice with 2×10^6 PFU of WE c54 intravenously led to a negligible

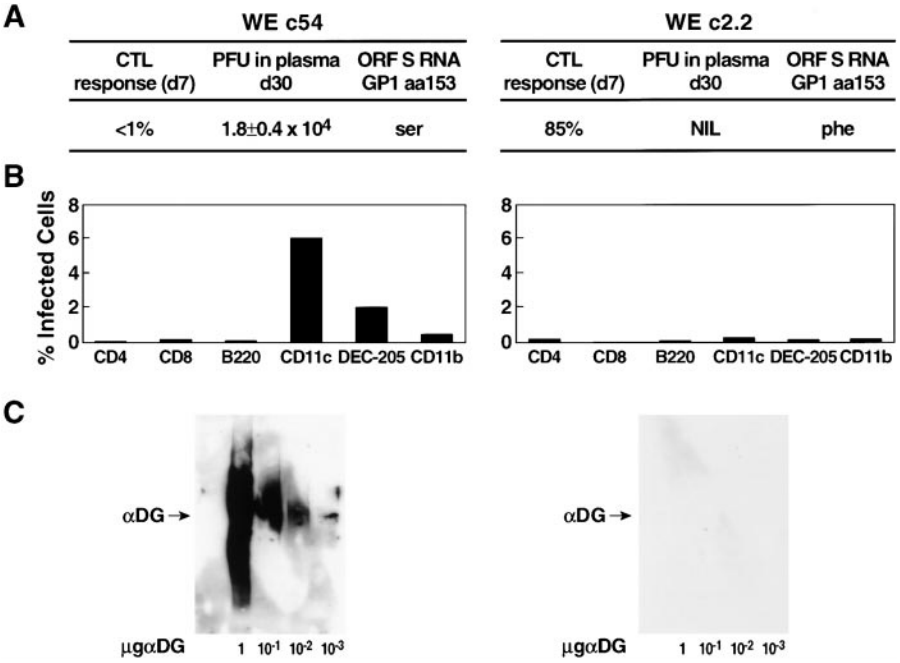

Figure 5. Comparison of binding affinities for the WE c54 and WE c2.2. isolates. (A) Biological properties of LCMV WE c54 and WE c2.2 as evaluated by the generation of an LCMV-specific CTL response at day 7 after infection and the ability or inability to clear the virus from the serum. CTL responses at day 7 are indicated as the percentage of ^{51}Cr release from BALB/c ByJ (H-2^d) targets at an effector/target ratio of 50:1, and the amount of infectious virus in serum is expressed as PFU per ml of plasma at day 30 after infection. The aa at position 153 of GP1 is indicated. (B) Comparison of the number of various splenic cell populations infected by LCMV WE c54 and WE c2.2. The results are shown as percentages of infected cells in each population as determined by FACS®. (A) VOPBA with decreasing amounts (1, 10^{-1}, 10^{-2}, and 10^{-3} μg) of purified α-DG blotted with 10^7 PFU of WE c54 or WE c2.2 virus detected with specific anti-GP LCMV antibodies as described in Materials and Methods. NIL, not detectable; ORF, open reading frame.

anti-LCMV CTL response 7 d after virus challenge and to the establishment of a persistent viral infection (Fig. 5 A). In contrast, mice given WE c2.2 virus generated an effective CTL response that cleared virus and terminated the infection 8 d after inoculation. Thus, WE c54 and WE c2.2 exhibited distinct CTL^-P^+ and CTL^+P^- phenotypes, respectively.

Reassortants between the two WE variants (WE c54 and WE c2.2) and ARM 53b mapped the CTL^-P^+ phenotype of WE c54 to the S RNA. Sequence analysis showed that the NPs of WE c54 and WE c2.2 were identical, but the GPs of these two viruses differed at a single aa position (WE c54 S153 and WE c2.2 F153) in GP1 (40). WE c54 bound with 3 logs higher affinity to α-DG than did WE c2.2 (Fig. 5 C). These results implicate, in addition to aa 260, aa 153 of GP1 in the binding of GP1 to α-DG. Experiments analyzing the anatomic distribution of WE c54 in the spleen after 3 d of virus infection showed that this CTL^-P^+ virus was restricted to the white pulp of the spleen. In contrast, WE c2.2 (CTL^+P^- phenotype) was found preferentially in the red pulp (data not show). FACS® analysis of cells obtained from the spleen showed that WE c54 but not WE c2.2 preferentially infected $CD11c^+$ and DEC-205^+ cells (Fig. 5 B).

Expression of α-DG in DCs. Replication of LCMV in $CD11c^+$ and DEC-205^+ DCs was associated with the CTL^-P^+ phenotype (Figs. 3–5, and Table I). The final experiment evaluated expression of α-DG in $CD11c^+$, $CD4^+$, $CD8^+$, and $B220^+$ cells. The lack of high affinity antibodies to DEC-205 prevented analysis of DEC-205^+ cells. Specific cell populations were isolated using high affinity cell type–specific antibodies coated on magnetic beads. Cells were lysed and α-DG enriched from solubilized total protein extract by microscale affinity purification using a jacalin–agarose matrix that preferentially binds to the mucin-type, O-linked glycans that are abundant on α-DG (41, 42). After the removal of unspecifically bound material, jacalin-bound glycoproteins were eluted and separated by SDS-PAGE, and subjected to VOPBA with LCMV Cl 13. LCMV binding activity was only detected in $CD11c^+$ cells (Fig. 6). Interestingly, comparing equivalent numbers of cells, the average signal of α-DG expression in total splenocytes was significantly lower then that of $CD11c^+$ cells (Fig. 6). This suggests that $CD11c^+$ cells represent a major cell population in the spleen expressing α-DG.

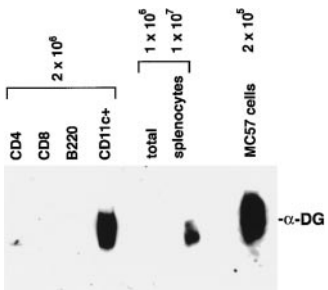

Figure 6. VOPBA with α-DG purified from fibroblasts (MC57 cells), total splenocytes, $CD4^+$, $CD8^+$, $B220^+$, or $CD11c^+$ cells incubated with LCMV Cl 13. α-DG purified from different numbers of cells (2×10^5 MC57 cells, 10^6 and 10^7 total splenocytes, and 2×10^6 $CD11c^+$, $CD4^+$, $CD8^+$, and $B220^+$ cells) was resolved in a 6% SDS-polyacrylamide gel. Incubation was with 10^8 PFU of Cl 13 and then with virus-specific antibody (see Materials and Methods). The arrow indicates the band corresponding to α-DG. The variability in molecular weights of α-DG from MC57 cells, total splenocytes, and $CD11c^+$ cells likely reflects different glycosylation patterns.

Discussion

This paper makes three important points. First, virus–DC interaction in vivo can be a leading event in the initiation of suppression of host immune response and the establishment of a persistent infection. Second, a crucial role of virus–receptor interaction is involved in the initiation of immunosuppression for LCMV and may be important for other viruses. Third, within the spleen, α-DG is highly expressed in $CD11c^+$ cells but not on $CD11b^+$, T, or B cells. We demonstrate that infection with strains and variants of LCMV that have a preferential tropism for DCs resulted in a suppression of the host immune system. Those viral variants with higher receptor affinity binding can be selected in vivo within the replicating viral quasispecies. Such selection results in the infection of DCs, which preferentially express the virus cellular receptor α-DG, leading to a generalized suppression of immune responses, including the anti-LCMV CTL response required for terminating the infection. Further, α-DG is expressed in high concentrations on $CD11c^+$ cells, and this molecule may serve as a useful marker in the segregation of DC populations.

Using mice whose immune system was compromised by different means allowed us to evaluate the selective pressures involved in the emergence of CTL^-P^+ viral variants. Virus isolates from lymphocytes and macrophages of CD4 ko, perforin ko, and TNF-α ko persistently infected mice exhibited a CTL^-P^+ phenotype when inoculated into adult immunocompetent mice. The CTL^-P^+ variants had an L or I in aa position 260 of GP1, instead of F found in the same position of CTL^+P^- viruses, implying the importance of this aa position in the selection of the CTL^-P^+ variants. As the same aa substitution of F→L/I at position 260 of GP1 was selected for in CD4 ko, perforin ko, and TNF-α ko mice, it is unlikely that selection of CTL^-P^+ variants is driven by the immune system. These viral variants are being produced in the replicating viral quasispecies and are able to adapt to favorable environments with the fittest of mutants chosen out from the viral quasispecies (43, 44). In vivo competition assays between ARM 53b and Cl 13 showed that Cl 13 has a higher fitness over ARM 53b for immune cells in the white pulp of the spleen (7, 10, 11). Our data indicate that those viral variants with increased binding receptor affinity may be selected from within the replicating viral quasispecies to bind to $CD11c^+$ and DEC-205^+ DCs. To our knowledge, this is the first in vivo report that selection occurs for viruses to enter specific cells such as the DC population. The selective pressure is likely based on the interaction of the virus with its receptor, thereby offering a marked advantage to the virus in initiating the dysfunction or destruction of the host professional antigen-presenting cells, thereby aborting the necessary host immune responses required to terminate the viral infection. By contrast and in other instances, selection

of viral variants by the host immune responses have been well established with influenza and HIV infections, providing an advantage to the virus over the host (for reviews, see references 45–47). Our observations are unique and different, as virus selection is based on virus receptor binding affinity to an essential cell involved in generating host immune responses, and this in turn aborts or reduces the basic adoptive host mechanism for controlling infection. This virus–DC type of selection in vivo may apply to other viruses that both cause immunosuppression or persistent infections and that infect/bind to DCs, i.e., HIV and measles.

The difference in tropism in the spleen between CTL^-P^+ and CTL^+P^- viral variants was remarkable. At day 7 after infection, almost 60% of DCs were infected by the CTL^-P^+ variants, making them excellent targets for the destruction by the host immune system. In contrast, 15% or less of DCs were infected by the CTL^+P^- variants at day 7 after infection according to the sensitivity of the assay, resulting in the majority of DCs being protected from either CTL lysis (7, 30) or direct viral effect on DC function (1, 2). The sustained replication of virus in $CD11c^+$ and enhanced replication in DEC-205^+ cells (>80% of such cells over the 2-wk observation period) suggest the possibility of ongoing infection of DCs migrating and repopulating the spleen. Experiments to analyze the kinetics of DC migration from the bone marrow, turnover and survival during LCMV infection, and functionality of infected DCs are currently under evaluation. Preliminary data suggest that the function of DCs, including expression of IL-12 and B7-1 (Sevilla, N., S. Kunz, and M.B.A. Oldstone, unpublished data) is affected by IS^+P^+ but not by IS^-P^- viruses.

In addition to the influence of a bulky aromatic aa (F) or a small aliphatic aa (L/I) in GP1 residue 260 in affinity binding to the LCMV cellular receptor α-DG, studies with CTL^-P^+ and CTL^+P^- WE virus variants indicated that the aromatic aa in GP1 residue 153 also prevented high affinity binding to α-DG. This was corrected by a substitution to S for F in GP1 aa 153. With the S in GP1 aa 153, WE strains bound at 2–3 logs higher affinity to α-DG and infected 20-fold more $CD11c^+$ and DEC-205^+ DCs than did the low affinity binding CTL^+P^- variant WE c2.2. These data suggest a generality in the DC–α-DG virus interactions for LCMV strains.

Our studies documented the high expression of α-DG on DCs. A comparison between total splenocytes and $CD11c^+$ cells indicated that $CD11c^+$ cells were the major cell expressing α-DG in the spleen. As shown in Fig. 6, sixfold fewer $CD11c^+$ cells had a fourfold enhanced concentration of α-DG over the amounts found in total spleen. Further, neither T, B, nor $CD11b^+$ cells expressed detectable amounts of α-DG. As no more than 1% of the total splenocytes are $CD11c^+$, the source of α-DG we observed in the total splenic population was due primarily to $CD11c^+$ cells.

DCs play a pivotal role in T cell activation and thus a critical role in initiating antiviral immunity (48). Studies with several DNA and RNA viruses (49–51) revealed that DCs are the most effective antigen-presenting cell for the stimulation of CTL responses. A cardinal feature of IDCs is the strong capacity to stimulate antigen-specific naive T cells to proliferate, secrete cytokines, and express CD40L (for a review, see reference 52). It would be a selective advantage for a virus to infect and impair the function of DCs. Such a scenario has been postulated to occur, based on in vitro studies with measles virus (53, 54), HIV (55, 56), and HSV-1 (57) infections. The studies presented here clearly document a selective advantage for a virus to directly interact with DCs in vivo, and provides a model system to dissect the molecules involved and the consequences of virus–DC interactions.

The authors thank Esteban Domingo and Claire F. Evans for invaluable discussions, Urs Christen for helping with FACS®, and Jeff Redwine for helping with the microscope.

This work was supported by National Institutes of Health grants AI09484, AI45927 (M.B.A. Odstone), and AG04342 (J.C. de la Torre). N. Sevilla was the recipient of a fellowship from the Human Frontier Science Program, S. Kunz received a fellowship from the Swiss National Science Foundation, A. Holz obtained funds from the Swiss National Science Foundation and the National Multiple Sclerosis Society, and D. Homann was the recipient of a fellowship from the Juvenile Diabetes Foundation International and was previously supported by National Institutes of Health training grant AG00080. K.P. Campbell is an investigator of the Howard Hughes Medical Institute. This is publication no. 13060-NP from the Department of Neuropharmacology, The Scripps Research Institute, La Jolla, California.

Submitted: 18 July 2000
Revised: 8 September 2000
Accepted: 19 September 2000

References

1. de la Torre, J.C., and M.B. Oldstone. 1996. Anatomy of viral persistence: mechanisms of persistence and associated disease. *Adv. Virus Res.* 46:311–343.
2. Oldstone, M.B. 1989. Viruses can cause disease in the absence of morphological evidence of cell injury: implication for uncovering new diseases in the future. *J. Infect. Dis.* 159: 384–389.
3. Fields, B.N., D.M. Knipe, and P.M. Howley. 1996. Persistance of viruses. *In* Virology. Lippincott-Raven, Philadelphia. 219–249.
4. McChesney, M.B., and M.B. Oldstone. 1989. Virus-induced immunosuppression: infections with measles virus and human immunodeficiency virus. *Adv. Immunol.* 45:335–380.
5. Doyle, M.V., and M.B. Oldstone. 1978. Interactions between viruses and lymphocytes. I. In vivo replication of lymphocytic choriomeningitis virus in mononuclear cells during both chronic and acute viral infections. *J. Immunol.* 121: 1262–1269.
6. Borrow, P., A. Tishon, and M.B.A. Oldstone. 1991. Infection of lymphocytes by a virus that aborts cytotoxic T lymphocyte activity and establishes persistent infection. *J. Exp. Med.* 174:203–212.
7. Borrow, P., C.F. Evans, and M.B.A. Oldstone. 1995. Virus-induced immunosuppression: immune system-mediated destruction of virus-infected dendritic cells results in generalized immunosuppression. *J. Virol.* 69:1059–1070.

8. Tishon, A., P. Borrow, C. Evans, and M.B. Oldstone. 1993. Virus-induced immunosuppression. 1. Age at infection relates to a selective or generalized defect. *Virology*. 195:397–405.
9. Ahmed, R., A. Salmi, L.D. Butler, J.M. Chiller, and M.B.A. Oldstone. 1984. Selection of genetic variants of lymphocytic choriomeningitis virus in spleens of persistently infected mice: role in suppression of cytotoxic T lymphocyte response and viral persistence. *J. Exp. Med.* 160:521–540.
10. Ahmed, R., and M.B.A. Oldstone. 1988. Organ specific selection of viral variants during chronic infection. *J. Exp. Med.* 167:1719–1724.
11. Evans, C.F., P. Borrow, J.C. de la Torre, and M.B. Oldstone. 1994. Virus-induced immunosuppression: kinetic analysis of the selection of a mutation associated with viral persistence. *J. Virol.* 68:7367–7373.
12. Dockter, J., C.F. Evans, A. Tishon, and M.B. Oldstone. 1996. Competitive selection in vivo by a cell for one variant over another: implications for RNA virus quasispecies in vivo. *J. Virol.* 70:1799–1803.
13. Matloubian, M., S.R. Kolhekar, T. Somasundarum, and R. Ahmed. 1993. Molecular determinants of macrophage tropism and viral persistence: importance of single amino acid changes in the polymerase and glycoprotein of lymphocytic choriomeningitis virus. *J. Virol.* 67:7340–7349.
14. Villarete, L., T. Somasundaram, and R. Ahmed. 1994. Tissue-mediated selection of viral variants: correlation between glycoprotein mutation and growth in neuronal cells. *J. Virol.* 68:7490–7496.
15. Matloubian, B., T. Somasundarum, S.R. Kolhekar, R. Selvakumar, and R. Ahmed. 1990. Genetic basis of viral persistence: single amino acid change in the viral polymerase affects ability of lymphocytic choriomeningitis virus to persist in adult mice. *J. Exp. Med.* 172:1043–1048.
16. Salvato, M., E. Shimomaye, P. Southern, and M.B. Oldstone. 1988. Virus-lymphocyte interactions. IV. Molecular characterization of LCMV Armstrong (CTL^+) small genomic segment and that of its variant, Clone 13 (CTL^-). *Virology*. 164:517–522.
17. Salvato, M., P. Borrow, E. Shimomaye, and M.B. Oldstone. 1991. Molecular basis of viral persistence: a single amino acid change in the glycoprotein of lymphocytic choriomeningitis virus is associated with suppression of the antiviral cytotoxic T-lymphocyte response and establishment of persistence. *J. Virol.* 65:1863–1869.
18. Cao, W., M.D. Henry, P. Borrow, H. Yamada, J.H. Elder, E.V. Ravkov, S.T. Nichol, R.W. Compans, K.P. Campbell, and M.B. Oldstone. 1998. Identification of alpha-dystroglycan as a receptor for lymphocytic choriomeningitis virus and Lassa fever virus. *Science*. 282:2079–2081.
19. Ibraghimov-Beskrovnaya, O., J.M. Ervasti, C.J. Leveille, C.A. Slaughter, S.W. Sernett, and K.P. Campbell. 1992. Primary structure of dystrophin-associated glycoproteins linking dystrophin to the extracellular matrix. *Nature*. 355:696–702.
20. Hemler, M.E. 1999. Dystroglycan versatility. *Cell.* 97:543–546.
21. Henry, M.D., and K.P. Campbell. 1999. Dystroglycan inside and out. *Curr. Opin. Cell Biol.* 11:602–607.
22. Parekh, B.S., and M.J. Buchmeier. 1986. Proteins of lymphocytic choriomeningitis virus: antigenic topography of the viral glycoproteins. *Virology*. 153:168–178.
23. Borrow, P., and M.B.A. Oldstone. 1992. Characterization of lymphocytic choriomeningitis virus-binding protein(s): a candidate cellular receptor for the virus. *J. Virol.* 66:7270–7281.
24. Dutko, F.J., and M.B. Oldstone. 1983. Genomic and biological variation among commonly used lymphocytic choriomeningitis virus strains. *J. Gen. Virol.* 64:1689–1698.
25. Buesa-Gomez, J., M.N. Teng, C.E. Oldstone, M.B. Oldstone, and J.C. de la Torre. 1996. Variants able to cause growth hormone deficiency syndrome are present within the disease-nil WE strain of lymphocytic choriomeningitis virus. *J. Virol.* 70:8988–8992.
26. Doyle, M.V., and M.B. Oldstone. 1978. Interactions between viruses and lymphocytes. I. In vivo replication of lymphocytic choriomeningitis virus in mononuclear cells during both chronic and acute viral infections. *J. Immunol.* 121: 1262–1269.
27. Buchmeier, M.J., and M.B. Oldstone. 1979. Protein structure of lymphocytic choriomeningitis virus: evidence for a cell-associated precursor of the virion glycopeptides. *Virology*. 99:111–120.
28. Kagi, D., B. Ledermann, K. Burki, P. Seiler, B. Odermatt, K.J. Olsen, E.R. Podack, R.M. Zinkernagel, and H. Hengartner. 1994. Cytotoxicity mediated by T cells and natural killer cells is greatly impaired in perforin-deficient mice. *Nature*. 369:31–37.
29. Rahemtulla, A., W.P. Fung-Leung, M.W. Schilham, T.M. Kundig, S.R. Sambhara, A. Narendran, A. Arabian, A. Wakeham, C.J. Paige, R.M. Zinkernagel, et al. 1991. Normal development and function of $CD8^+$ cells but markedly decreased helper cell activity in mice lacking CD4. *Nature*. 353:180–184.
30. Tishon, A., P.J. Southern, and M.B. Oldstone. 1988. Virus-lymphocyte interactions. II. Expression of viral sequences during the course of persistent lymphocytic choriomeningitis virus infection and their localization to the L3T4 lymphocyte subset. *J. Immunol.* 140:1280–1284.
31. King, C.C., R. de Fries, S.R. Kolhekar, and R. Ahmed. 1990. In vivo selection of lymphocyte-tropic and macrophage-tropic variants of lymphocytic choriomeningitis virus during persistent infection. *J. Virol.* 64:5611–5616.
32. Austyn, J.M., and S. Gordon. 1981. F4/80, a monoclonal antibody directed specifically against the mouse macrophage. *Eur. J. Immunol.* 11:805–815.
33. Holz, A., N. Schaeren-Wiemers, C. Schaefer, U. Pott, R.J. Colello, and M.E. Schwab. 1996. Molecular and developmental characterization of novel cDNAs of the myelin-associated/oligodendrocytic basic protein. *J. Neurosci.* 16:467–477.
34. Oldstone, M.B., H. Lewicki, D. Thomas, A. Tishon, S. Dales, J. Patterson, M. Manchester, D. Homann, D. Naniche, and A. Holz. 1999. Measles virus infection in a transgenic model: virus-induced immunosuppression and central nervous system disease. *Cell.* 98:629–640.
35. Rodriguez, M., M.J. Buchmeier, M.B. Oldstone, and P.W. Lampert. 1983. Ultrastructural localization of viral antigens in the CNS of mice persistently infected with lymphocytic choriomeningitis virus (LCMV). *Am. J. Pathol.* 110:95–100.
36. Tishon, A., M. Eddleston, J.C. de la Torre, and M.B.A. Oldstone. 1993. Cytotoxic T lymphocytes cleanse viral gene products from individually infected neurons and lymphocytes in mice persistently infected with lymphocytic choriomeningitis virus. *Virology*. 197:463–467.
37. Odermatt, B., M. Eppler, T.P. Leist, H. Hengatner, and R.M. Zinkernagel. 1991. Virus-triggered acquired immunodeficiency by cytotoxic T-cell-dependent destruction of anti-

gen-presenting cells and lymph follicle structure. *Proc. Natl. Acad. Sci. USA.* 88:8252–8256.
38. Metlay, J.P., M.D. Witmer-Pack, R. Agger, M.T. Crowley, D. Lawess, and R.M. Steinman. 1990. The distinct leucocyte integrins of mouse spleen dendritic cells as identified with new hamster monoclonal antibodies. *J. Exp. Med.* 171:1753–1771.
39. Jiang, W., W.J. Swiggard, C. Heufler, M. Peng, A. Mirza, R.M. Steinman, and M.C. Nussenzweig. 1995. The receptor DEC-205 expressed by dendritic cells and thymic epithelial cells is involved in antigen processing. *Nature.* 375:151–155.
40. Teng, M.N., P. Borrow, M.B. Oldstone, and J.C. de la Torre. 1996. A single amino acid change in the glycoprotein of lymphocytic choriomeningitis virus is associated with the ability to cause growth hormone deficiency syndrome. *J. Virol.* 70:8438–8443.
41. Chiba, A., K. Matsumura, H. Yamada, T. Inazu, T. Shimizu, S. Kusunoki, I. Kanazawa, A. Kobata, and T. Endo. 1997. Structures of sialylated O-linked oligosaccharides of bovine peripheral nerve alpha-dystroglycan. The role of a novel O-mannosyl-type oligosaccharide in the binding of alpha-dystroglycan with laminin. *J. Biol. Chem.* 272:2156–2162.
42. Ervasti, J.M., A.L. Burwell, and A.L. Geissler. 1997. Tissue-specific heterogeneity in alpha-dystroglycan sialoglycosylation. Skeletal muscle alpha-dystroglycan is a latent receptor for *Vicia villosa* agglutinin b4 masked by sialic acid modification. *J. Biol. Chem.* 272:22315–22321.
43. Holland, J.J., J.C. de la Torre, and D.A. Steinhauer. 1992. RNA viral population as quasispecies. *Curr. Top. Microbiol. Immunol.* 176:1–20.
44. Domingo, E., and J.J. Holland. 1997. RNA virus mutations and fitness for survival. *Annu. Rev. Microbiol.* 51:151–178.
45. Scholtissek, C. 1994. Source for influenza pandemics. *Eur. J. Epidemiol.* 10:455–458.
46. Gupta, S., and R.M. Anderson. 1999. Population structure of pathogens: the role of immune selection. *Parasitol. Today.* 15: 497–501.
47. Borrow, P., H. Lewicki, X. Wei, M.S. Horwitz, N. Peffer, H. Meyers, J.A. Nelson, J.E. Gairin, B.H. Hahn, M.B. Oldstone, and G.M. Shaw. 1997. Antiviral pressure exerted by HIV-1-specific cytotoxic T lymphocytes (CTLs) during primary infection demonstrated by rapid selection of CTL escape virus. *Nat. Med.* 3:205–211.
48. Banchereau, J., and R.M. Steinman. 1998. Dendritic cells and the control of immunity. *Nature.* 392:245–252.
49. Kast, W.M., C.J. Boog, B.O. Roep, A.C. Voordouw, and C.J. Melief. 1988. Failure or success in the restoration of virus-specific cytotoxic T lymphocyte response defects by dendritic cells. *J. Immunol.* 140:3186–3193.
50. Hengel, H., M. Lindner, H. Wagner, and K. Heeg. 1987. Frequency of herpes simplex virus-specific murine cytotoxic T lymphocyte precursors in mitogen- and antigen-driven primary in vitro T cell responses. *J. Immunol.* 139:4196–4202.
51. Nonacs, R., C. Humborg, J.P. Tam, and R.M. Steinman. 1992. Mechanisms of mouse spleen dendritic cell function in the generation of influenza-specific, cytolytic T lymphocytes. *J. Exp. Med.* 176:519–529.
52. Steinman, R.M., M. Pack, and K. Inaba. 1997. Dendritic cells in the T-cell areas of lymphoid organs. *Immunol. Rev.* 156:25–37.
53. Schneider-Schaulies, S., and V. ter Meulen. 1999. Pathogenic aspects of measles virus infections. *Arch. Virol. Suppl.* 15:139–158.
54. Servet-Delprat, C., P.O. Vidalain, H. Bausinger, S. Manie, F. Le Deist, O. Azocar, D. Hanau, A. Fischer, and C. Rabourdin-Combe. 2000. Measles virus induces abnormal differentiation of CD40 ligand-activated human dendritic cells. *J. Immunol.* 164:1753–1760.
55. Rubbert, A., C. Combadiere, M. Ostrowski, J. Arthos, M. Dybul, E. Machado, M.A. Cohn, J.A. Hoxie, P.M. Murphy, A.S. Fauci, and D. Weissman. 1998. Dendritic cells express multiple chemokine receptors used as coreceptors for HIV entry. *J. Immunol.* 160:3933–3941.
56. Knight, S.C., and S. Patterson. 1997. Bone marrow-derived dendritic cells, infection with human immunodeficiency virus, and immunopathology. *Annu. Rev. Immunol.* 15:593–615.
57. Kruse, M., O. Rosorius, F. Kratzer, G. Stelz, C. Kuhnt, G. Schuler, J. Hauber, and A. Steinkasserer. 2000. Mature dendritic cells infected with herpes simplex virus 1 exhibited inhibited T-cell stimulatory capacity. *J. Virol.* 74:7127–7136.